Resource-saving microprocessor-based reed switch current protection

Mark Kletsel , Bauyrzhan Mashrapov [*], Rizagul Mashrapova

Department of Electric Power Industry Toraighyrov University, Lomov str., 64, Pavlodar 140008 Kazakhstan

A B S T R A C T

We suggest designing a cutoff and an overcurrent protection for 6–35 kV electrical installations with switchgear cubicles on the basis of reed switches and a microprocessor without current transformers. A reed switch is a small glass tube with plates inside, which contact under the action of the corresponding magnetic field. Two reed switches are mounted near each busbar inside a switchgear cubicle at a safe distance using specially designed structures. The magnetic induction which acts on them is determined by the Biot–Savart law with experimentally found coefficients. The effect of currents in neighboring electrical installations and in switchgear cubicle casings is taken into account. We have developed and describe here an algorithm of protection operation and a technique for selecting parameters and estimating protection sensitivity. Such protections are noise-resistant due to detection of short circuits by the third actuation of a read switch; they detect a failed component with the help of built-in diagnostics. The test diagnostics is performed by means of supplying current simultaneously to the control windings of two reed switches, and the functional diagnostics, by means of supplying current to them in turn. The efficiency of such protections is confirmed by the simulation results.

1. Introduction

Overcurrent protection and current cutoff make up the vast majority of all relay protection devices. Like other protections [1], they usually receive information from current transformers (CT[1]). These CTs contain high-quality copper, steel, and insulating materials in amounts dozens and even hundreds of times higher than the protection devices. In addition, they have unacceptable errors under high short-circuit (SC) currents. Therefore, the problem of getting rid of CT and designing protections on the basis of new sensors is considered a fundamentally unsolved problem in the electric power industry, which has been repeatedly pointed out during CIGRE sessions [2,3]. For some electrical installations (EI), protections without CTs and with magnetically sensitive elements, such as induction coils [4], Rogowski coils [3,5,6], Hall sensors [7,8], and reed switches [9–13], have already been suggested. For electrical installations with switchgear cubicles, which are the most common in 6–35-kV networks, only centralized reed switch protection [14] and differential busbar protection based on Rogowski coils [15–17] are suggested. Works [14,15] describe only the principle of constructing protection devices. Works [16,17] present the circuit and simulation results, however, without taking into account the effect of currents in a

neighboring electrical installation and switchgear cubicle housings on the output signal of a Rogowski coil. The disadvantages of the devices in [15–17] are the need in high-voltage insulation and large size of the current sensor in comparison with other magnetically sensitive elements. The purpose of this work is to create overcurrent protection and cutoff based on reed switches without CTs for an electrical installation with switchgear cubicles.

Reed switches have been chosen because a reed switch can simultaneously function as a current sensor, a current relay, and an analog-to-digital converter. In additions, they transmit signals via control circuits, but not measuring circuits, which is very important for relay protections.

2. Reed switch and its parameters

A reed switch (Fig. 1) is a sealed glass tube (1) (0.5–5 cm long and 0.3–0.5 cm diameter) with metal plates (2) inside. It is mounted at a safe distance h from busbar 3. A magnetic field (MF) with the induction B_{lon} (produced by the current I) acts along the reed switch contacts. It is activated (closes contacts) if $B_{lon} = B_{act} = \mu_0 F_{act}/l_c$, where μ_0 is the permeability of vacuum, B_{act} is the actuation induction; F_{act} is the magnetomotive force of the reed switch actuation determined at the manufacturing plant with the use of a control winding with the reed

---

Nomenclature

B_{act}	actuation induction of reed switch [T]
B_{lon}	induction acts along the reed switch contacts [T]
B_A	field induction produced by current in phase A [T]
B_{po}	induction of the protection operation [T]
B_{P1}- B_{P4}	inductions of fields acting on the reed switch in modes 1–4 [Тл]
B_{po1}-B_{po4}	inductions of the protection operation adjusted according to modes 1–4 [T]
B_1- B_3	inductions of fields roduced by the self-start currents of EM 1, 2, 3 [T]
$B_1^{(2)}, B_3^{(2)}$	inductions of fields produced by the fault current contributions from EM1 and EM3 [T]
$B_2^{(1.1)}$	inductions of field produced by the amplitude of the total current in busbar C of the switchgear cubicle with EM2 [T]
B_{fc2}	inductions of field produced by the amplitude of the self-start current in phase A of EM2 [T]
B_{SCmin}	inductions of field produced by the minimal SC current [T]
k_{adj}	adjusting factor
k_1	correction factor responsible for errors caused by the effect of the current type, busbar shape, and metal elements of switchgears
k_{n1}	factor which consider the shielding effects of the casings of neighboring and protected switchgear cubicles
k_s	sensitivity coefficient
I_A, I_B, I_C	current in phases A, B, C of EI [A]

$I_{ss1}, I_{ss2}, I_{ss3}$	amplitudes of self-start currents of EM1, 2, 3 [A]
$I_2^{(3)}$ $(I_2^{(2)})$	amplitude of the three-phase (two-phase) SC current at EM2 [A]
$I_2^{(1.1)}$	sum of the fault current at two points and fault current contributions from EM 1, 3, 4 [A]
$I_3^{(1.1)}$	sum of the fault current at two points and fault current contributions from EM 1, 2, 4 in phase A [A]
F_{op}	magnetomotive force of the reed switch actuation [A]
l_c	winding length [m]
h_A, h_B, h_C (h_{A1}, h_{B1}, h_{C1} and h_{A2}, h_{B2}, h_{C2}, and h_{A3}, h_{B3}, h_{C3})	the distances from the axes of phases A, B, and C (of a switchgear cubicle under study and left and right neighbor switchgear cubicles) to the center of gravity of a reed switch [m]
μ_0	magnetic constant [H/m]
t_{et1}	protection time delay [s]
t_{et2}	time lag between diagnostic checks [s]
t_{et3}	time required for operation of the protection logic and the output element [s]
t_{et4}	duration of diagnostics of reed switch 2 [s]
$\alpha_A, \alpha_B, \alpha_C$ (α_{A1}, α_{B1}, α_{C1} and α_{A2}, α_{B2}, α_{C2} and α_{A3}, α_{B3}, α_{C3})	duration of diagnostics of reed switch 2 [s] angles between the longitudinal axis of a reed switch and the induction vector of MF produced by the currents in phase A, B, and C (of a switchgear cubicle under study and right and left neighbors)
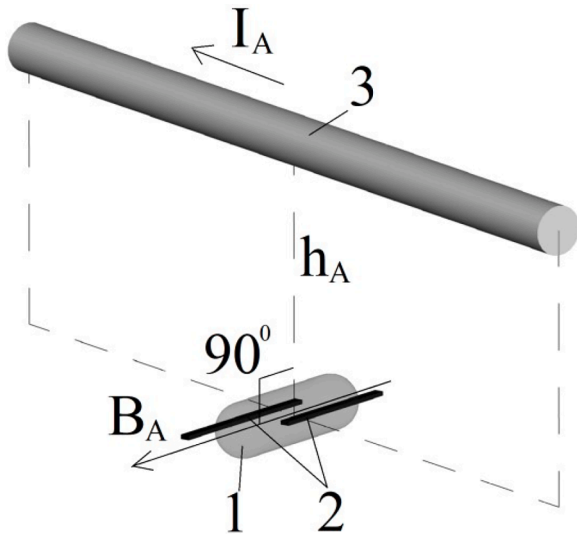
Fig. 1. Arrangement of a reed relay near a busbar (single column).

relay wrap length l_c.

The reed switch operates twice for the power frequency cycle, and the time of its actuation $t_{act} \leq 3$ ms depending on the amplitude B_{lon}. To determine the current in the electrical installation phase the reed switch is triggered at (Fig. 1), one can use the simplest form of the Biot–Savart law, but with the correction factor k_{e1} (experimentally determined). It is introduced because this law is true for direct current flowing through a thin and long conductor. In addition, there are switchgear cubicle casings, partitions in them (screens), and errors in installing the reed switch at a given point. Hence, for the reed switch to operate, the current I_A in the phase A (Fig. 1), at which the reed switch operates, should satisfy the

equality

$$k_{e1}\frac{\mu_0 I_A}{2\pi h_A}cos\alpha_A = \frac{\mu_0 F_{act}}{l_c}.$$

where h_A is the distance between the axes of the phase A and the center of gravity of the reed switch; α_A is the angle between the longitudinal axis of the reed switch and the MF induction vector ($\alpha_A = 0$ in Fig. 1, since $B_{lon} = B_A$).

In three-phase electrical installations, a reed switch is affected by MFs produced by currents of all phases. Then,

$$B_{lon} = \frac{\mu_0}{2\pi}\left(\frac{I_A}{h_A}cos\alpha_A + \frac{I_B}{h_B}cos\alpha_B + \frac{I_C}{h_C}cos\alpha_C\right),$$

where I_B and I_C are the currents in phases B and C of the electrical installation; h_B and h_C are the distances between the axes of phases B and C and the center of gravity of the reed switch; α_B and α_C are angles between the longitudinal axis of the reed switch and the MF induction vectors induced by the currents I_B and I_C.

3. Reed relay protection circuit and algorithm of its operation

Reed switches 1 and 2 (Fig. 2) with contacts 3 and 4 and control windings 5 and 6 are mounted near an electrical installation phase like in Fig. 1. They are actuated at the same current in this phase. Microcontroller unit 7 is connected to the contacts; the output element of the protection (OE), indication block 8, ac voltage sources (ACS) 9 and 10, OE deactivation block 12, automatic switching button 13, and test diagnostics starting and stopping block 14 are connected to the microcontroller; ACS 11 is connected to block 14. Everything is exactly the same for phase C.

Microcontroller unit 7 operates according to the algorithm shown in Fig. 3 (patent [18] has been obtained for the logic scheme of the algorithm without test diagnostics). Here, t_{et1} is the protection time delay; t_{et2} is the time lag between self-diagnostic checks ($t_{et2} = 43$ h is
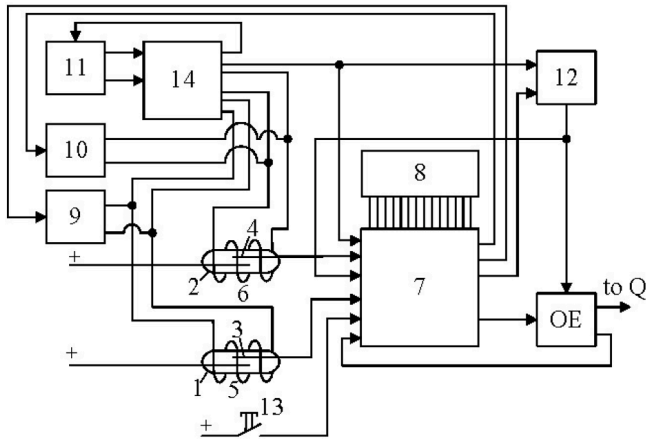
Fig. 2. Block diagram of the self-tested current protection (single column).

considered optimal [19]). Reed switches 1 and 2 should produce three pulses before a short circuit is detected. This is necessary for the protection to fail in the case of noise of up to 0.02 s in duration.

After setting up the protection and putting it into operation, the electrical installation breaker is closing. Button 13 is pressed. Self-diagnostics starts. Voltage from source 9 is applied to winding 5 of reed switch 1, and the circuit between OE and the electrical installation breaker Q is interrupted by block 12 (Fig. 2). If the device is properly functioning, then voltage is applied to the OE and is removed from winding 5 and applied to winding 6 of reed switch 2. All this takes the time t_{et3}, which is required for operation of the protection logic and OE. If reed switch 2 is actuated and breaks for the time t_{et4} (the time of reed switch 2 diagnostics), then it properly operates, and the diagnostics stops. Voltage is again applied to winding 5 in time t_{et2}. If a failure is detected, then the diagnostics signals about it. The protection is disabled.

In the event of a short-circuit in the electrical installation, both reed switches are simultaneously actuated, block the diagnostics, and start the protection logic. The electrical installation is turned off. During test diagnostics, staff starts block 14, the electrical installation trip circuit is broken by block 12, and voltage is applied to the reed switch windings. Then, the above described procedure is performed.

4. Selection of electrical installation protection and cutoff actuation parameters

Let power cables to electric motors (EMs) go from the switchgear. Points the closest to busbars but at a safe distance are selected for mounting. Then the protection actuation parameters are calculated. The principle of operation of the overcurrent protection suggested is the same as of traditional ones; therefore, it should not operate under the action of a MF produced by the self-start currents of Ems. It is also necessary to take into account the effect of MF produced (Fig. 4) by currents in the busbars of neighboring switchgears (2 to the left and 3 to the right) in the followiing modes: (1) self-starting, (2) three-phase SC, (3) two-phase SC, and (4) double ground faults. Hence, the induction B_{po} of the overcurrent protection operation should be adjusted according to the induction of MFs acting on the reed switch in these four modes (P), i. e., $B_{po1} = k_{adj}B_{P1}$, $B_{po2} = k_{adj}B_{P2}$, $B_{po3} = k_{adj}B_{P3}$, and $B_{po4} = k_{adj}B_{P4}$.

Let us consider inductions B_{P1}–B_{P4}. All EM of a section (Fig. 4) can simultaneously self-start; therefore,

$$B_{P1} = B_1 + B_2 + B_3 = k_{e1}\mu_0 G_1 I_{ss1} + k_{e1}k_1\mu_0 G_2 I_{ss2} + \\ + k_{e1}k_1\mu_0 G_3 I_{ss3} = k_{e1}\mu_0 G_1 I_{ss1}(1 + k_2 k_3 + k_4 k_5), \tag{1}$$

where

$$G_1 = \frac{\cos\alpha_{A1}}{2\pi h_{A1}} + \frac{\cos\alpha_{B1}}{2\pi h_{B1}}e^{j240} + \frac{\cos\alpha_{C1}}{2\pi h_{C1}}e^{j120}; \tag{2a}$$

$$G_2 = \frac{\cos\alpha_{A2}}{2\pi h_{A2}} + \frac{\cos\alpha_{B2}}{2\pi h_{B2}}e^{j240} + \frac{\cos\alpha_{C2}}{2\pi h_{C2}}e^{j120}; \tag{2b}$$

$$G_3 = \frac{\cos\alpha_{A3}}{2\pi h_{A3}} + \frac{\cos\alpha_{B3}}{2\pi h_{B3}}e^{j240} + \frac{\cos\alpha_{C3}}{2\pi h_{C3}}e^{j120}; \tag{2c}$$
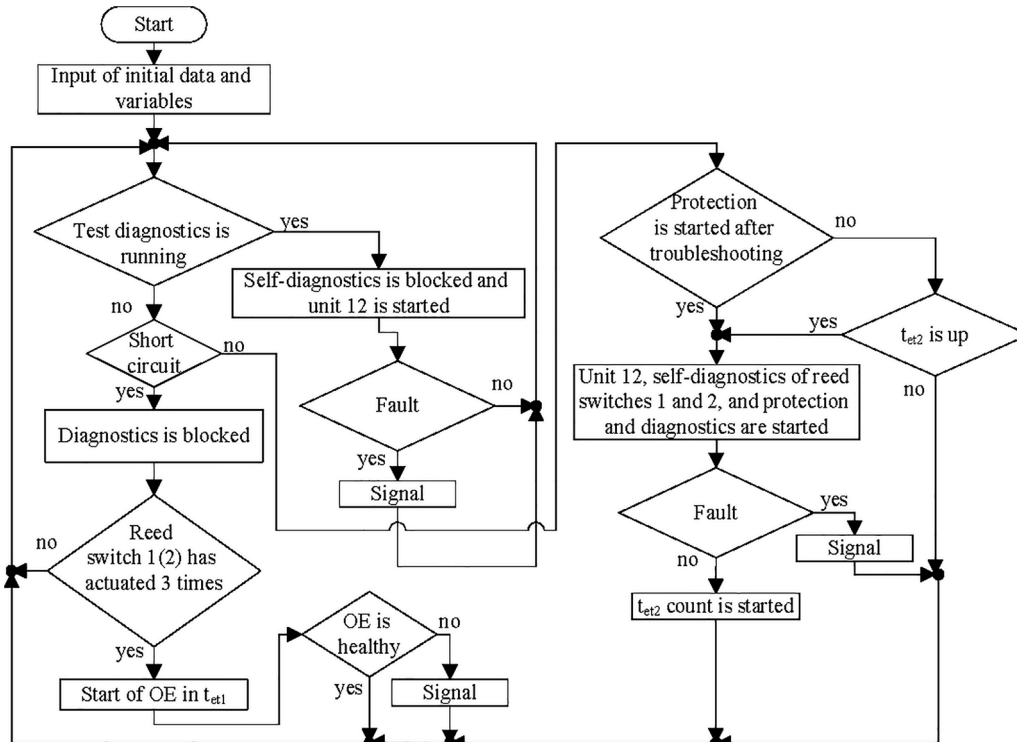
Fig. 3. Algorithm of operation of the protection device suggested (1.5-column).
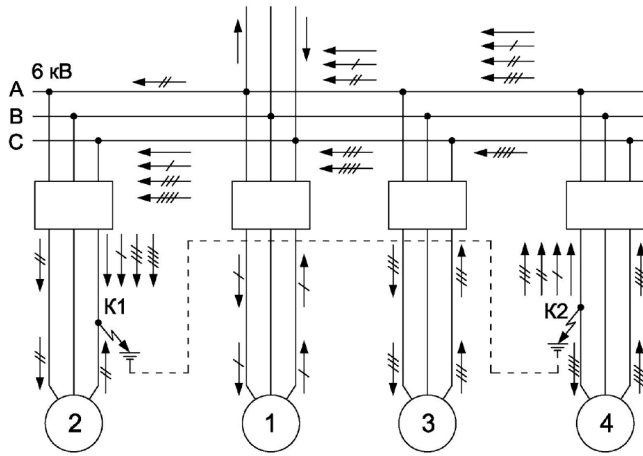
Fig. 4. Directions of fault currents (crossed arrows) and double ground fault currents (uncrossed arrows) in terminals (single column).

$$k_2 = \frac{I_{ss2}}{I_{ss1}}; \tag{2d}$$

$$k_3 = \frac{k_1 G_2}{G_1}; \tag{2e}$$

$$k_4 = \frac{I_{ss3}}{I_{ss1}}; \tag{2f}$$

$$k_5 = \frac{k_1 G_3}{G_1}; \tag{2g}$$

B_1, B_2, and B_3 are the resulting vectors of MF inductions acting along the reed switch axis and produced by the self-start currents of EM1, EM2, and EM3; k_{e1} is the factor responsible for the errors caused by effect of current type, shape of busbar, and metal components of a switchgear the reed switch are fixed inside, and inaccuracy of their mounting; k_1 is the factor which consider the shielding effects of the casings of neighboring and protected switchgear cubicles; I_{ss1}, I_{ss2}, and I_{ss3} are the amplitudes of self-start currents of EM1, EM2, and EM3; the subscript «1» («2», «3») means that the current relates to the switchgear cubicle EM1 (2, 3) is connected to; they do not relate to the factors k and inductions B_P and B_{po}; α_{A1}, α_{B1}, and α_{C1} (α_{A2}, α_{B2}, and α_{C2} and α_{A3}, α_{B3}, and α_{C3}) are the angles between the longitudinal axis of the reed switch and the induction vector of MF produced by the current in phase A, B, and C of a switchgear cubicle under study (right and left neighbors) directed from the busbars; h_{A1}, h_{B1}, and h_{C1} (h_{A2}, h_{B2}, and h_{C2} and h_{A3}, h_{B3}, and h_{C3}) are the distances from the axes of busbars of phases A, B, and C of the corresponding switchgear cubicles to the center of gravity of the reed switch.

Under the condition of fault-current contribution from EM1 and EM3 to points of three-phase or two-phase SC at EM2 and considering the fault current contribution to be equal to the self-start current and, in the worst case, to coincide in phase with the SC current, the induction B_{P2} or B_{P3}, calculated like B_{P1}, affects the reed switch. In this case, the current I_{ss2} in Eq. (1) is replaced by the amplitude of the three-phase (two-phase) SC current $I_2^{(3)}$ ($I_2^{(2)}$). When calculating B_{P2}, the angles α are increased by $180°$ (fault currents in the three phases are directed to the busbars). When calculating B_{P3}, G_1, G_2, and G_3 are replaced by $G_1^{(2)}$, $G_2^{(2)}$, and $G_3^{(2)}$, which are calculated by Eq. (2), where only the terms corresponding to damaged phases remain, with a minus sign between them (opposite currents), and without factors e^{j120} and e^{j240}.

In the case of double ground fault (Fig. 4), for example, at K1 on phase C of EM2 and K2 on phase A of EM4, all EMs switch to the generator mode. Therefore, the currents in these phases are directed like in Fig. 4. Neglecting currents in undamaged phases and analyzing the

current directions (Fig. 4), we find that all these currents have the greatest effect on the reed switch fixed near phase A of EM1 (Fig. 4), i.e.,

$$B_{P4} = B_1^{(2)} + B_2^{(1.1)} + B_{fc2} + B_3^{(2)} = k_{e1}\mu_0 G_1^{(2)} I_{ss1}(1 + k_6 k_7 + k_2 k_8 + k_4 k_9), \tag{3}$$

where $B_1^{(2)}$ and $B_3^{(2)}$ are the inductions of MFs produced by the fault current contributions from EM1 and EM3, calculated like in the case of two-phase SC; $B_2^{(1.1)}$ and B_{fc2} are the inductions of MFs produced by the amplitude of the total current $I_2^{(1.1)}$ (sum of the fault current at two points and fault current contributions from EM1, EM3, and EM4) in busbar C of the switchgear cubicle with EM2 and the amplitude of the self-start current I_{ss2} in phase A of EM2, which affect the reed switch; $G_2^{(1.1)} = \frac{\cos\alpha_{C2}}{2\pi h_{C2}}$; $G_{fc2} = \frac{\cos\alpha_{A2}}{2\pi h_{A2}}$; $k_7 = \frac{k_1 G_2^{(1.1)}}{G_1^{(2)}}$; $k_8 = \frac{k_1 G_{fc2}}{G_1^{(2)}}$; $k_9 = \frac{k_1 G_3^{(2)}}{G_1^{(2)}}$; $k_6 = \frac{I_2^{(1.1)}}{I_{ss1}}$.

If the ground fault points are at EM2 and EM3, then the MF induction B_{P5} along the reed switch axis is calculated by Eq. (3), where $G_3^{(2)}$ is replaced by $G_{fc3} = -\cos\alpha_{C3}/2\pi h_{C3}$ ("–" indicates that the currents (Fig. 4) in the switchgear damaged are oppositely directed) and the term $k_{e1}k_1\mu_0 G_3^{(1.1)} I_3^{(1.1)}$ is introduced ($G_3^{(1.1)} = -\cos\alpha_{A3}/2\pi h_{A3}$). The fourth term in Eq. (3) is omitted for the protection of the last terminal (EM4).

To determine the coefficients k_{e1}, k_3, k_5, k_7, k_8, and k_9 for switchgears K-630 and K-2–10 (switchgear cubicles manufactured in Russia are currently used in Kazakhstan), experiments were carried out. Depending on the damage type, the same currents from 200 to 600 A were supplied to one, two, or three phases of the switchgear cubicles of the protected and neighboring terminals. The MF inductions were measured (Fig. 5) with the use of inductance coils (IC) 2 mounted instead of reed switches on plate 3 fixed at draw-out element 4 at convenient points 1. The center of gravity of IC 2 was spaced $l_1 = 0.14$–0.2 M apart from the plane of busbars 5 between right 6 and left 7 walls of the switchgear ($l_2 = 0.9$ m), and the longitudinal axis of IC 2 was arranged as shown in Fig. 5. The above coefficients were calculated from the ratios of the MF inductions measured at the same point inside the switchgear under study (determined for each switchgear type during adjustment).

Fig. 6a shows the MF inductions B_{E1} and B_{E2} which act along the longitudinal axis of IC 2 as functions of the distance l between wall 6 and IC 2 point under busbar currents of 600 A and $l_1 = 0.14$ m. Fig. 6b shows the inductions B_{E3}, B_{E4}, and B_{E5} produced by the same currects in the busbars of the neighboring switchgear from the side of wall 6. Here, B_{E1} and B_{E2} correspond to B_1 and $B_1^{(2)}$; B_{E3}, to $B_2^{(1.1)}$ and B_{fc2}; B_{E4}, to B_2 and B_3; and B_{E5}, to $B_3^{(2)}$. The wave-like dependences of B_{E1} and B_{E2} on l in Fig. 6a is explained by variations in angles α and distances h during
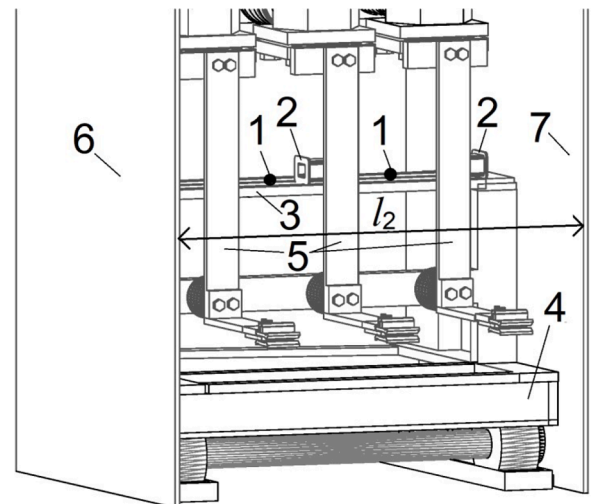
Fig. 5. Arrangement of reed switches (inductance coils 2) inside a switchgear cubicle (single column).
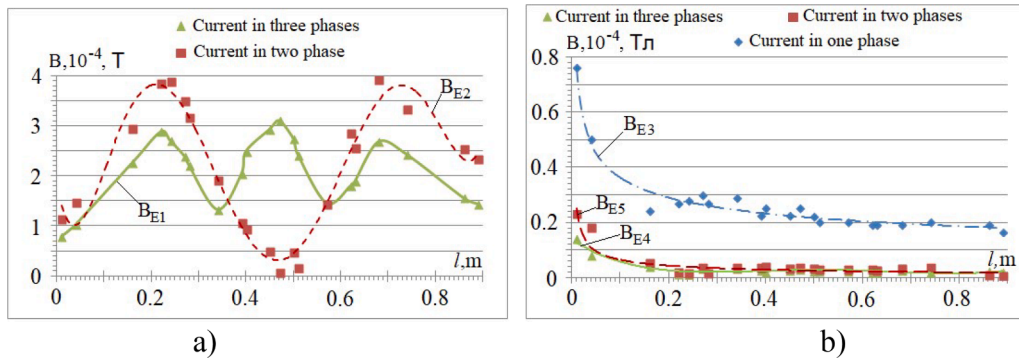
Fig. 6. Inductions of MFs produced by currents in busbars of (a) considered and (b) neighboring switchgear as functions of l (single column).

displacement of IC 2.

The analysis of the results has shown the following.

1. Reed switches should be mounted at distances $l \geq 0.22$ m from the switchgear walls in front of phases A, B, and C. The coefficient $G_1^{(2)}$ is calculated for the reed switches near the phases A and B for a short circuit between them, and for the reed switch near phase B, for a short circuit between B and C or A and B.

2. The reed switch is maximally affected by the induction of the MF produced by the current only in the neighboring switchgear phase the closest to IC 2 (B_{E3} in Fig. 6b). Therefore, the conservative value $k_7 = k_8 = B_{E3}/B_{E2}$ was taken when calculating B_{P4} and B_{P5} ($B_{E3}/B_{E2} = 0.08$ at the point $l = 0.22$). The values of the coefficients k_3, k_5, and k_9 are equal to B_{E4}/B_{E1} and B_{E5}/B_{E2} (B_{E4} is the MF induction affecting the reed switch in the case of three-phase SC in the neighboring switchgear, and B_{E5}, in the case of two-phase SC). They did not exceed 0.01 in the experiments, and k_{e1} did not exceed 0.42.

To avoid the protection operation in the modes under study, the protection should be adjusted by the maximal of inductions B_{P4}–B_{P5}. According to (3), induction B_{P4} is maximal. Therefore,

$$B_{po} \geq k_{tune-out}B_{P4}. \tag{4}$$

The current cutoff tripping induction is also adjusted by the induction created by the maximal SC current at the end of the object protected.

Protection sensitivity and speed. The protection sensitivity is checked, as in a traditional one, by calculating the sensitivity coefficient k_s, but changing currents to the MF produced by them:

$$k_s = \frac{B_{SCmin}}{B_{po}} \geq 1.5, \tag{5}$$

where B_{SCmin} is the MF induction which affects the reed switch under minimal SC current (at the end of a line for lines; at the beginning, for cutoff, and $k_s = 2$; B_{SCmin} is calculated under SC on busbars from which the line starts; B_{SCmin} for transformers, under SC at the low voltage terminals, for the cutoff, at high voltage terminal, for EM, at its terminals from the side of the supply cable). Examples of calculation of B_{po} and assessment of k_s are given in the Appendix.

For current cutoff, t_{cutoff} is the sum of the delay $t_d = 0.02$ s, required for ensuring the noise immunity, and the response time of the reed switch (up to 3 ms) and of the output relay (0.015 s [20]). The protection operates in 38 ms, which meets modern requirements (for example, the response time of the Siemens MICOM P115 relay can attain 40 ms [21]). As for the overcurrent protection, its time delay is chosen in the same way as the traditional one.

5. Test results

The operability of the overcurrent protection was verified in simulation in the MatLab environment. The results are shown in Fig. 7. Reed switches 1 and 2 are not actuated in the electrical installation load mode. However, as soon as the protection is switched on by pressing button 13 (see Fig. 2), self-diagnostics starts, and pulses from reed switch 1 (Fig. 7a) and a pulse from block 12, which prevents tripping the electrical installation (EI) breaker, appear. These pulses are t_{et3} long, for example, 0.7 s. The protection operates in time t_{et1}, for example, 0.5 s, after the start, unit 7 starts the output element (OE), and a pulse appears (Fig. 7a). The EI breaker is not tripped. At the time point 0.8 s, diagnostics of reed switch 1 and overcurrent protection stops and diagnostics of reed switch 2 begins. At the time point 0.9 s, it stops, and the protection returns to its original state. During test diagnostics (Fig. 7b), signals are produced by reed switches 1 and 2 and unit 12. The diagnostics stops after operation of OE.

In the case of a SC during self-diagnostics (Fig. 7b), for example, at the time point 0.3 s, reed switches 1 and 2 are simultaneously activated, and block 12 stops signaling. At the time point 0.81 s, the output element operates, and the EI is switched off. In the case of SC between self-diagnostic checks (Fig. 7c), the device operates in the same way.

If, for example, reed switch 1 fails to operate during a short circuit in the EI (Fig. 7d), its malfunction is detected in 0.02 s, and a signal (pulse) is produced. The output element operates in t_{et1} and the EI is turned off. If contacts 3 of reed switch 1 are sealing during a short circuit (Fig. 7e), a signal indicating its malfunction is produced. The output element operates in time t_{et1}, the EI is turned off, and the protection is blocked to prevent its false operation when the EI is again turned on.

The protection operation in the case of malfunction of its logic, OE, and elements of the diagnostic circuit was tested in a similar way. The protection worked correctly in all those events. This allows us to assume properly functioning of the suggested current protection.

6. Structures for reed switch mounting in switchgears [22]

They are made without metal parts and allow changing the reed switch position so as to conveniently change the protection operation parameters. Let us consider one of the simplest structure [22]. It (Fig. 8) includes plate 1 with reed switches 2, plates 3, 4, and 5 (two last are with a scale, they are inserted in holes in plate 1 and attached to bar 10), rod 6 with thread 7 and handle 8 built-in at one end into hollow cylinder 9, and at the other end, into plate 1. Cylinder 9 is attached to bar 10, bar 10, to plate 3, and plate 3, to the switchgear cubicle (above plate 3 in Fig. 5). Plate 1 is perpendicular to the plane of the busbar cross section, and reed switches 2 are mounted at certain angles to this plane. The protection operation parameters are controlled by moving plate 1 along plates 4 and 5 and selecting appropriate reed switch 2.
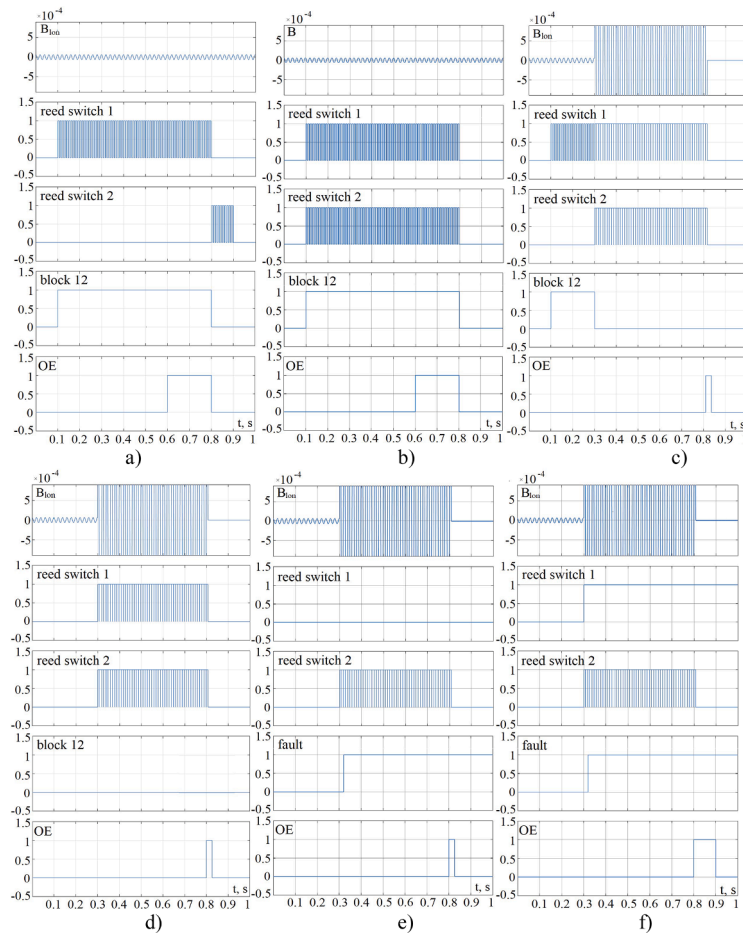
Fig. 7. Oscillograms of induction B_{lon} and signals from reed switches 1 and 2, OE, and block 12 under (a, b) the load and (c-f) a short circuit (2- column).
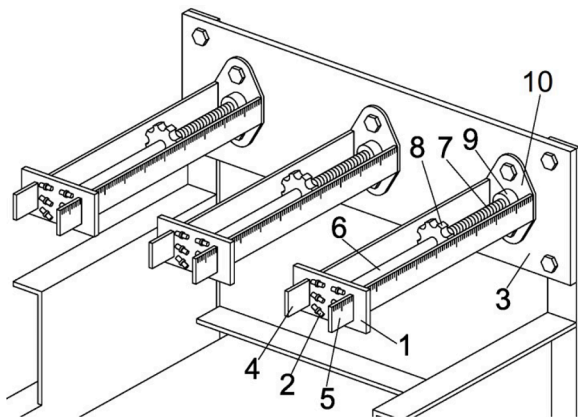
Fig. 8. Structure for mounting reed switches in a switchgear (single column).

7. Estimated resource saving due to use of the protection suggested

Table 1 shows the mass and size parameters of the protection suggested and an ABB protection with three CSs. The total mass for 110 V includes the mass of the external insulator.

This table shows that traditional protections require 6 and 15 times more copper and steel than our protection for 6 kV, 14 and 32 times more for 10 kV, and 37 and 80 times more for 35 kV. In addition, traditional protections require 15–230 kg of high-voltage insulation (depending on the voltage class), which is not needed for our protection.

Table 1

Mass and size parameters of the ABB protection with 3 CTs (numerator) and the protection suggested (denominator).

| Voltage, kV | Mass, kg | | | | Total volume, m³ |
	Total	Cu	steel	insulation	
6	33/4	3/0.5	15/1	14/-	0.022/0.007
10	80/4	7/0.5	32/1	31/-	0.024/0.0075
35	390/8	22/0.6	120/1.5	230/-	1.9/0.025

The analysis of similar data for the protections made by several other companies has shown similar ratios.

8. Results, their significance and discussion

8.1. Results

Microprocessor overcurrent protection and cutoff are created for the first time for 6–35-kV electrical installations on the basis of reed switches, which simultaneously function as current transformers and current relays. The device circuit, the algorithm of its operation, the technique for selecting settings, and the structure for mounting reed switches have been developed. Oscillograms of signals from a reed switch, the protection output element, and its blocking element are presented, as well as of the induction of magnetic fluxes, produced by busbar current, which act on a reed switch during a short circuit in an electrical installation both in the load operation mode during functional and test diagnostics and in the case of malfunction of one of reed switches.

8.2. Significance of the results

1. When manufacturing such a protection system for a switchgear with current sensors, 6–37 times smaller amount of copper and 15–80 times smaller amount of steel are required, and there is no need in rare earths.
2. The protection operation algorithm and the technique for selecting the protection actuation parameters developed contribute to the development of the relay protection theory: the algorithm allows tuning out from magnetic interference by means of waiting for the third activation of a reed switch, as well as detecting malfunctions. The technique makes it possible to use the simplest formula of the Biot–Savart law.
3. The protections designed make it possible to maximize the reliability (theoretically, by dozens of times) of the entire relay protection system for networks with a voltage of 6–35 kV by duplicating protection with CTs and CTs themselves by the majorization principle (CTs are currently not duplicated).

8.3. Discussion

The obtained patent for the device design confirms its novelty. The usefulness of the device is obvious. Protections are not inferior in speed to protections of most famous companies (the cutoff we suggest operates in 38 ms, while a Siemens MICOM P115 relay actuates in 40 ms [21]). We assume the protections to be no worse in reliability as well owing to the duplication of reed switches and built-in test and functional diagnostics. High reliability is also provided by the control of the proper operation of functional diagnostics. The simulation of the protection operation in diagnostic and short circuit modes and in the events of faults in these modes confirms its performance. There is no need in high qualification and much time to determine the coefficients for the simplest formula of the Biot–Savart law. However, the sensitivity of protection can be insufficient in some cases because of a need in tuning out from the effect on reed switches of magnetic fluxes produced by currents in neighboring EIs, including by seed currents from EMs connected to neighboring EIs. The sensitivity can be increased by mounting a screen; however, this requires additional research. Another disadvantage is a need in designing different structures for mounting reed switches for different switchgear types, though the structure we suggest is simple and convenient. Indeed, CTs also depend on the switchgear type.

9. Conclusions

The created current cutoff and reed switch overcurrent protection contribute to the solution of the fundamentally unsolved problem in the electric power industry, that is, the design of protections without current transformers, and to enhancement of the relay protection reliability. They meet the speed requirements, and there is reason to believe (see "Results and Discussion") the same for reliability. As for sensitivity, it can be insufficient in some cases. The developed technique for selecting protection parameters can be easily learned by average workers. Simulation has confirmed that the protection performs all suggested functions.

Funding

CRediT authorship contribution statement

Mark Kletsel: Conceptualization, Methodology, Data curation, Writing – original draft, Funding acquisition. **Bauyrzhan Mashrapov:** Conceptualization, Methodology, Validation, Investigation, Writing – original draft, Writing – review & editing, Funding acquisition. **Rizagul Mashrapova:** Software, Validation, Investigation.

Declaration of competing interest

The authors declare that they have no known competing financial interests or personal relationships that could have appeared to influence the work reported in this paper.

Data availability

All data generated or analysed during this study are included in this published article

Acknowledgements

Supplementary materials

Supplementary material associated with this article can be found, in the online version, at doi:10.1016/j.epsr.2024.110276.

References

[1] J. Das, Power systems protective relaying, CRC Press, Boca Raton, 2018.
[2] A. D'yakov, World electrical energy in the beginning of the 21st century (By meaterials of the 39th CIGRESession, Paris), Energetika za Rubezhom 4–5 (2004) 44–45.
[3] L. Kojović, Non-conventional instrument transformers for improved substation design, CIGRE Session 46 (2016).
[4] A. Novozhilov, D. Assainova, N. Zhumataev, T. Novozhilov, Switched magnetic current transformer, Russ. Electr. Engin. 42 (2022) 579–582, https://doi.org/ 10.3103/S1068798X2206017X.
[5] B. Li, M. Wen, X. Shi, L. Wang, Y. Chen, An improved distance relay based on electronic transformer by using instantaneous value after equal transfer processes, IET Gener. Transm. Distrib. 16 (2022) 2501–2512, https://doi.org/10.1049/ gtd2.12469.
[6] E. Esmail, A. Almalaq, K. Alqunun, Z. Ali, S. Aleem, Rogowski coil-based autonomous fault mana gement strategy using karen bell transformation for earthed active distribution networks, Ain Shams Eng. J. 14 (2022) 101953, https:// doi.org/10.1016/j.asej.2022.101953.
[7] M. Crescentini, S. Syeda, G. Gibiino, Hall-effect current sensors: principles of operation and implementation techniques, IEEE Sens. J. 22 (2022) 10137–10151, https://doi.org/10.1109/JSEN.2021.3119766.
[8] S. Ranasingh, T. Pradhan, D. Koteswara Raju, A. Singh, A. Piantini, An approach to wire-wound hall-effect based current sensor for offset reduction, IEEE Sens. J. 22 (2022) 2006–2015, https://doi.org/10.1109/JSEN.2021.3133105.
[9] A. Zhantlesova, M. Kletsel, P. Mayshev, B. Mashrapov, D. Issabekov, New filters for symmetrical current components, Int. J. Electr. Power Energy Syst. 101 (2018) 85–91, https://doi.org/10.1016/j.ijepes.2018.03.005.
[10] J. Teng, S. Luan, W. Huang, D. Lee, Y. Huang, A cost-effective fault management system for distribution systems with distributed generators, Int. J. Electr. Power Energy Syst. 65 (2015) 357–366, https://doi.org/10.1016/j.ijepes.2014.10.029.
[11] P. Zahlmann, J. Birkl, T. Bohm, K. Buehler, J. Maget, A. Ehrhardt, E. Shulzhenko, Germany Patent 102018111308-B3, May 09, 2019.
[12] A. Barukin, A. Berguzinov and O. Talipov, Mounting measuring devices of reed switch protection near conductors of electrical installations, in: 2020 International Multi-Conference on Industrial Engineering and Modern Technologies (FarEastCon), Vladivostok, Russia, 2020, https://doi.org/10.1109/FarEastCon502 10.2020.9271569.
[13] A. Barukin, A. Kaltayev and Y. Lenkov, Majority voting schemes of differential protections without current transformers with functional diagnostics for converting units and electric motors, in: 2020 International Conference on Industrial Engineering, Applications and Manufacturing (ICIEAM), Sochi, Russia, 2020, https://doi.org/10.1109/ICIEAM48468.2020.9112078.
[14] Hemant K. Mody. US Patent 20030128035 A1, Jul. 10, 2003.
[15] L. Kojovic, M.T. Bishop, Field experience with differential protection of power transformers based on Rogowski coil current sensors, *in: Actual Trends Development of Power System Protection and Automation*, vol. 7–10, Moscow, Russia, 2009, September.
[16] D.B. Solovev, S.S. Kuzora, Implementation of noise-immune Rogowski coils for busbar differential protection modernization, Electric Power Syst. Res. 140 (2016) 965–975, https://doi.org/10.1016/j.epsr.2016.03.039.

[17] A.H. Abdulwahid, Sh. Wang, A busbar differential protection based on fuzzy reasoning system and Rogowski-coil current sensor for microgrid, in: 2016 IEEE PES Asia-Pacific Power and Energy Engineering Conference (APPEEC), Xi'an, China, 2016, https://doi.org/10.1109/APPEEC.2016.7779496.

[18] B. Mashrapov, Republic of Kazakhstan patent 35675, May 20, 2022.

[19] R. Billinton, M. Fotuhi-Firuzabad, T. Sidhu, Determination of the optimum routine test and self-checking intervals in protective relaying using a reliability model,

IEEE Trans. Power Syst. 17 (2002) 663–669, https://doi.org/10.1109/MPER.2002.4312392.

[20] https://rele.ru/catalog/rele-promezhutochnye-puskateli-kontaktory/rele-promezhutochnye/r3.html (accessed 09 February 2024).

[21] MiCOM P115, Manual (global file) P115/EN M/C43, 2015.

[22] Kletsel, M., Berguzinov, A., Mashrapov, B., Talipov, O. Russian federation patent 2584548, May 20, 2016.